Asymmetric Ratchet Effect for Directional Transport of Fog Drops on Static and Dynamic Butterfly Wings

Chengcheng Liu,[†] Jie Ju,[‡] Yongmei Zheng,[†,*] and Lei Jiang[†,‡,*]

[†]Key Laboratory of Bio-Inspired Smart Interfacial Science and Technology of Ministry of Education, School of Chemistry and Environment, Beihang University, Beijing, 100191, People's Republic of China, and [‡]Beijing National Laboratory for Molecular Sciences (BNLMS), Institute of Chemistry, Chinese Academy of Sciences, Beijing 100190, People's Republic of China

ABSTRACT Inspired by novel creatures, researchers have developed varieties of fog drop transport systems and made significant contributions to the fields of heat transferring, water collecting, antifogging, and so on. Up to now, most of the efforts in directional fog drop transport have been focused on static surfaces. Considering it is not practical to keep surfaces still all the time in reality, conducting investigations on surfaces that can transport fog drops in both static and dynamic states has become more and more important. Here we report the wings of *Morpho deidamia* butterflies can directionally transport fog drops in both static and dynamic states. This directional drop transport ability results from the micro/nano ratchet-like structure of butterfly wings: the surface of butterfly wings is composed of overlapped scales, and the scales are covered with porous asymmetric ridges. Influenced by this special structure, fog drops on static wings are transported directionally as a result of the fog drops' asymmetric growth and coalescence. Fog drops on vibrating wings are propelled directionally due to the fog drops' asymmetric dewetting from the wings.

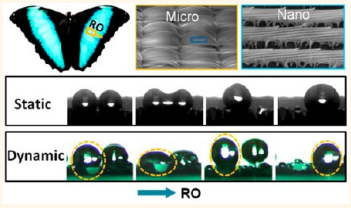

KEYWORDS: static · dynamic · butterfly wings · directional transport · fog drops

Biological surfaces with special structures show attractive fog drop transport abilities.[1−5] Inspired by the surfaces of organisms such as one-dimensional cactus spines,[1] spider silk,[2] and two-dimensional hydrophobic/hydrophilic desert beetle backs,[3] researchers have fabricated varieties of materials used for fog drop transport, which have made great contributions to both academic and industrial applications.[6−9] Up to now, directional fog drop transport has been realized on static surfaces with various charactersitcs,[1,2,6−10] while reports on materials that could transport fog drops in both static and dynamic states are still rare. Considering surfaces of many essential infrastructures such as air conditioners, aircraft, and power lines do not always work in static conditions, finding a surface that can directionally transport fog drops in both static and dynamic states has become more and more imperative.

Wings of butterflies exhibit static and vibrating states in daily life.[11−13] No matter in which state, butterflies need light-loaded wings to ensure their flying flexibility.[14−17] Therefore, driving fog drops away from the wings becomes necessary. *Morpho* butterflies live in the rainforest with high humidity all year. A previous investigation has found the wings of *Morpho* butterflies exhibit directional adhesion, which causes drops deposited on the wings to roll off along one direction easily with the help of gravity.[14] Different from deposited drops, fog drops will grow and coalescence, which makes the mechanisms for the propulsion of fog drops special. In this work, we find the wings of *Morpho deidamia* butterflies can drive fog drops away from the surfaces in both static and dynamic states without the assistance of gravity. Static butterfly wings transport fog drops directionally owing to the asymmetric drop growth and coalescence on the micro/nano ratchet-like structure of the wings. Dynamic butterfly wings transport fog drops directionally due to the fog drops' asymmetric dewetting from the micro/nano ratchet-like structure triggered by vibration. An optimal vibration mode that could propel fog drops in a large-diameter range is found. Our work opens a door for the fabrication of two-dimensional surfaces serving for the directional fog drop transport in both static and dynamic conditions, which

* Address correspondence to zhengym@buaa.edu.cn; jianglei@iccas.ac.cn.

Received for review September 10, 2013 and accepted January 7, 2014.

Published online January 07, 2014
10.1021/nn404761q

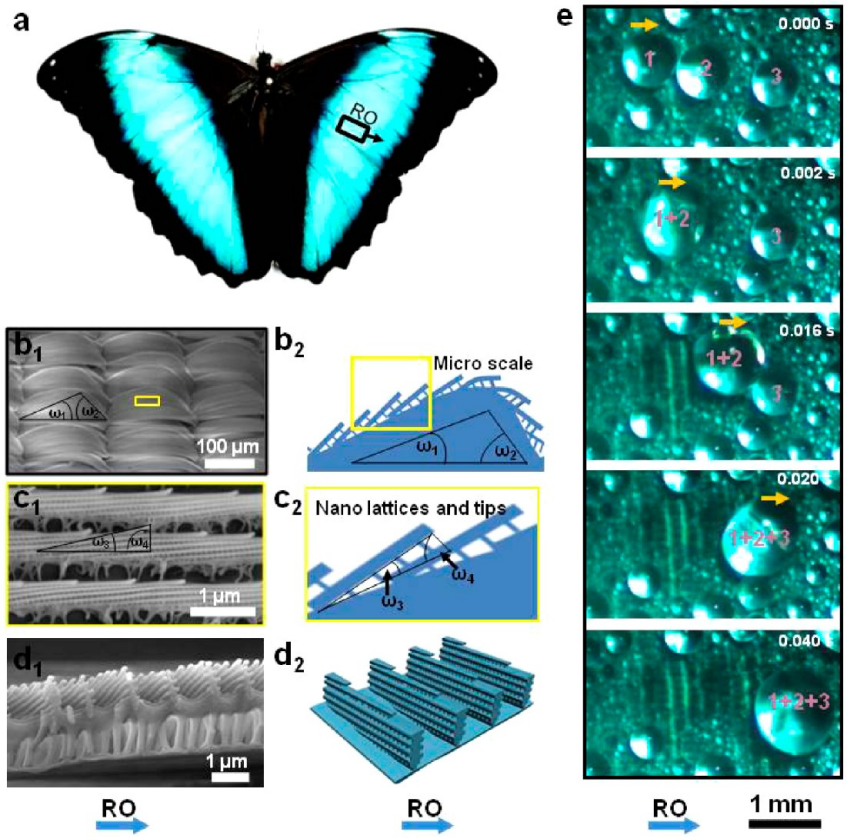

Figure 1. (a) Photo of a *Morpho deidamia* butterfly. The black arrow indicates the radial outside (RO) direction of the wing. (b_1) Oblique view ESEM image of the overlapped scales on butterfly wings as indicated by the black square in (a). (c_1) Oblique view ESEM image of the ridges on the scale as indicated by the yellow square in (b_1). (d_1) Cross section view ESEM image of ridges on the scale. (b_2–d_2) Illustrations of the micro/nanoratchet-like structure of butterfly wings. (e) Directional transport of fog drops on a static butterfly wing observed from the top view (the video rate was 500 f/s). Yellow arrows indicate the movement direction of the fog drops.

has practical significance in fluid-controlling tasks such as heat transferring, antifogging, and water harvesting.

RESULTS AND DISCUSSION

The wings of *M. deidamia* show typical anisotropic superhydrophobicity. On the wings, the water contact angle was 151.3° ± 0.4° (the optical image is shown in Figure S1 in the Supporting Information), and the water rolling-off angle (RA) was 5.0° ± 1.9° along the radial outside (RO) direction of the wing and 18.3° ± 1.0° against the RO direction (Figure 1a, RO direction is indicated by the black arrow), respectively.

The surface of the butterfly wing consists of overlapped scales with a length of ~200 μm and a width of ~150 μm. The scales bend toward the surface (oblique view and top view environmental scanning electron microscope (ESEM) images are shown in Figure 1b_1 and Figure S2b, respectively), and the tilt angle along the RO direction (ω_1) is smaller than that against the RO direction (ω_2) (as illustrated by Figure 1b_2). On the surface of a scale, there are parallel ridges with nanotips tilting toward the RO direction (oblique view and top view ESEM images are shown in Figure 1c_1 and Figure S2c, respectively). The tilt angle of the tip along the RO direction (ω_3) is smaller than that against the RO direction (ω_4) (as illustrated by Figure 1c_2). Microscales and nanotips make the surface exhibit an asymmetric ratchet-like structure, which leads to the anisotropic wetting property of the wings.[14] Ridges are formed by about six layers of stacked cuticle lamellae. The cuticle lamella is composed of lattices with a thickness of ~75 nm and a width of ~50 nm (Figure 1c_1,d_1), which renders a porous structure on the ridge (as illustrated by Figure 1d_2). Nanolattices and microscales enhance the surface roughness, which leads to the superhydrophobicity of the wings.[18,19]

Directional fog drop transport on static butterfly wings is shown in Figure 1e. In fog, neighbor drops (*e.g.*, drop 1 and drop 2) coalesced into drop 1+2 (at 0.002 s). Drop 1+2 kept its movement along the RO direction and swept other drops (*e.g.*, drop 3) on its way, triggering new coalescence (at 0.020 s). Then drop 1+2+3 continued to move directionally.

The detailed behaviors of fog drops on butterfly wings are helpful to reveal the mechanisms of directional drop transport on static wings. It is found that the behaviors of fog drops can be divided into three stages: in the first stage (Figure 2a), the fog drop of

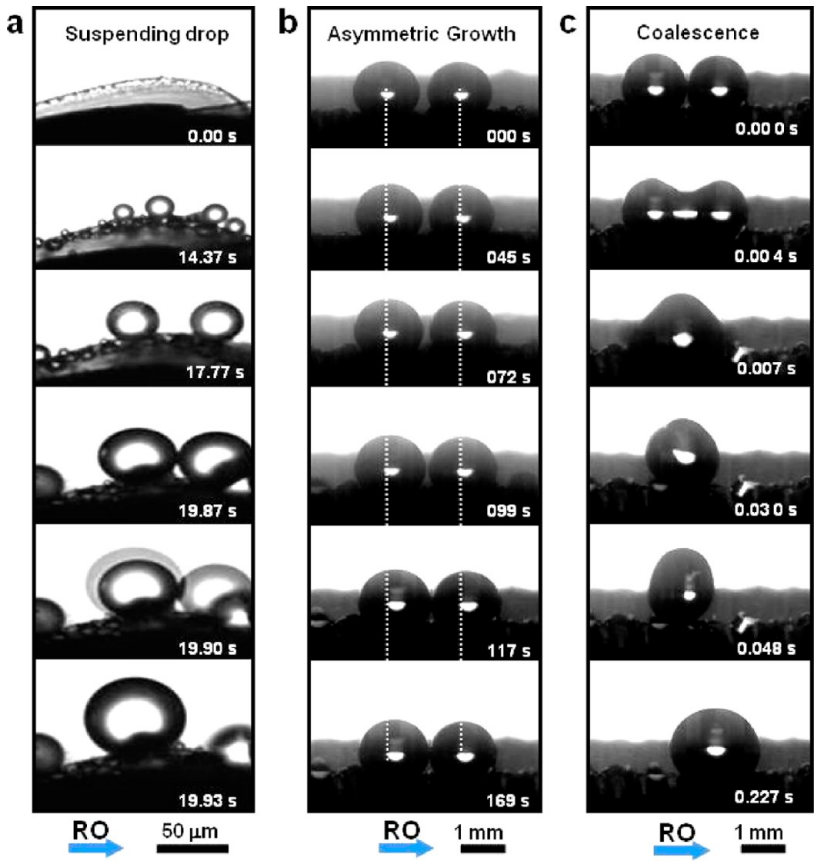

Figure 2. Sequential optical images of side views showing the directional fog drop transport on static butterfly wings (the start time was set as 0 s at each stage). (a) Growth and coalescence of drops on a single scale. (b) Directional transport of growing fog drops that were larger than the size of a single scale. The centers of the white dotted lines overlapped with the drop gravity centers at 000 s. (c) Directional transport of coalescent drops that were larger than the size of a single scale (the video rate was 1000 f/s).

size ~1 μm exhibited a semispherical shape (14.37 s). As the diameter grew, the fog drop of size ~5 μm showed a spherical shape and was suspended on top of the ridges (17.77 s). The suspended state was confirmed by the air trapped in the grooves between the ridges (as indicated by the light area in Figure S3b).[20] After being suspended on the ridges, the fog drop grew stably (from 17.77 to 19.87 s). When neighbor drops contacted each other (19.87 s), coalescence happened. The right drop was absorbed by the left one (from 19.87 to 19.93 s), showing a movement direction that was opposite that of the RO direction. In our repeated experiments, the absorbed drops moved without uniform direction and coalescent drops showed no obvious motion. In the second stage (Figure 2b, the fog drops were larger than the size of a single scale), the fog drops grew on the butterfly wing and advanced along the RO direction (from 45 to 169 s). At the third stage (Figure 2c), coalescence happened between drops that were larger than the size of a single scale. At the moment of coalescence, a liquid bridge formed between neighbor drops and the initial parts of the drops moved toward each other (0.004 s). After that the coalescent drop impacted (0.007 s) and contracted asymmetrically (0.030 s) from the surface. Then it observably advanced along the RO direction (from 0.048 to 0.227 s).

We explained the behaviors of fog drop transport on static wings in terms of wettability and energy law based on the asymmetric micro/nanoratchet-like structure, as illustrated in Figure 3. At the first stage (Figure 3a), drop 1′ and drop 2′ are smaller than the distance between the ridges, so they spread in the grooves and exhibit a semispherical shape. Because of the roughness effect of the structure, the surface of the scale exhibits robust superhydrophobicity.[18,19] Thus with increasing volume, drop 1′ and drop 2′ grow out of the grooves, and finally the grown drop 1 and drop 2 become suspended on the ridges. Because drop 1′ is located more deeply in the groove than drop 2′, the grown drop 1 has a larger fraction of liquid/solid interface, which leads to its larger retention force.[21] Therefore, drop 1 absorbs its neighbor drop 2 with smaller retention force, and the coalescent drop 1+2 shows no obvious motion.

In the second stage (Figure 3b), air pockets in the grooves between the ridges (Figure S3b) and crevices among the scales (Figure S4b) greatly reduce the

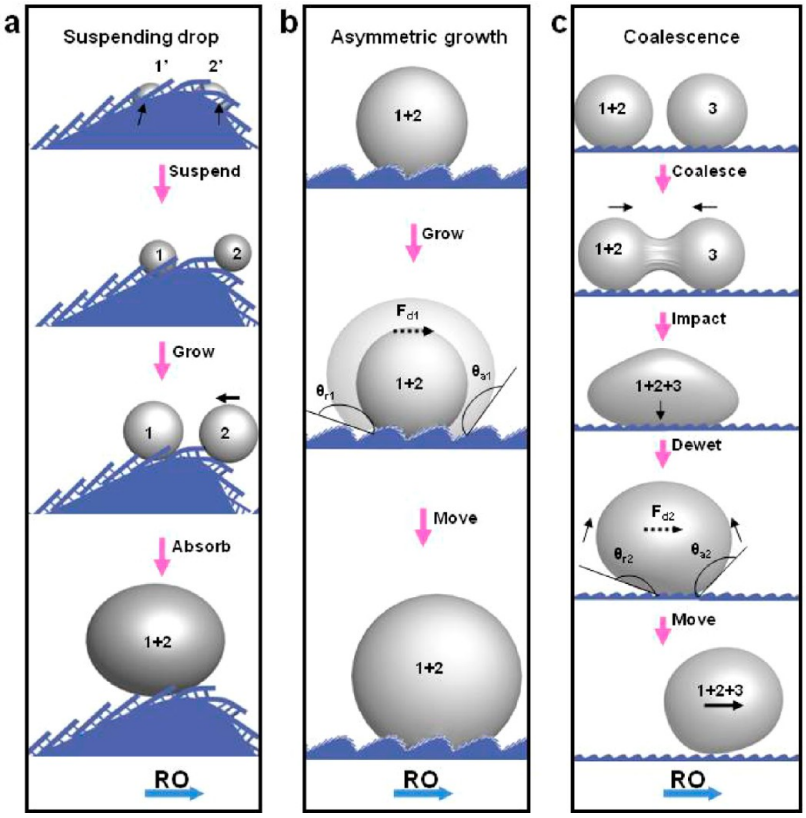

Figure 3. Illustrations of the behaviors of fog drops on static butterfly wings. (a) Growth and coalescence of drops on a single scale. (b) Directional transport of a growing fog drop that is larger than the size of a single scale. (c) Directional transport of a coalesced fog drop that is larger than the size of a single scale. The black arrows indicate the flow direction of the inner fluid of a fog drop.

fraction of liquid/solid interface. Thus the fog drop at this stage has a relatively smaller retention force and is easy to drive.[21] When growth starts, the right side of drop 1+2 grows along the RO direction, and it encounters a smaller retention force in this direction because of the smaller tilt angles of the scales (ω_1) and tips (ω_3).[22] The smaller retention force makes the right side of the drop 1+2 spread easily along the RO direction and air takes less space under it. In the opposite direction, the left side of the drop grows against the RO direction. The larger tilt angles of the scales (ω_2) and tips (ω_4) make the left side of the drop not easy to spread and more air is trapped under it. Therefore as for drop 1+2, the increase of the advancing angle (θ_{a1}, at the right side of the drop) is smaller than the increase of the receding angle (θ_{r1}, at the left side of the drop). Thus drop 1+2 exhibits an asymmetric shape, which leads to an imbalance of the surface tension forces acting on the two opposite sides of the drop.[23] The net surface tension force the entire drop experiences is written as[10]

$$F_{d1} = \int_{L_{left}}^{L_{right}} \gamma(\cos\theta_{a1} - \cos\theta_{r1})dl \qquad (1)$$

where γ is the surface tension of water and dl is the integrating variable along the length from the right to the left side of the drop. When $\theta_{a1} < \theta_{r1}$, F_{d1} points to the RO direction and increases with the drop growth as a result of the increasing difference between θ_{a1} and θ_{r1}. When F_{d1} is larger than the retention force the entire drop encounters in the RO direction, it will propel drop 1+2 directionally. At this stage, by tuning the ratchet angles (ω_1, ω_2, ω_3, and ω_4) of the asymmetric ratchet-like structure, drops with different volumes would encounter different retention forces in these two opposite directions.[22,24] Thus the motion of the growing fog drop can be controlled.

At the third stage (Figure 3c), the capillary force introduced by the liquid bridge makes the initial parts of mother drops move toward each other.[25] The continuous movement of inner fluid makes coalescent drop 1+2+3 impact and subsequently dewet from the surface. In the deweting process, the left side of the drop dewets along the RO direction, but the right side dewets against the RO direction. The asymmetric drop shape (Figure 2c, 0.030 s) reveals the drop encounters a smaller adhesive force when dewetting along the RO direction but a larger adhesive force when dewetting against the RO direction. This difference most prabably results from the relative discontinuous three-phase contact line along the RO direction, while a relative continuous or quasi-continuous three-phase contact

line against the RO direction is influenced by the asymmetric ratchet-like structure.[14] Since drop 1+2+3 dewets easily along the RO direction, the increase of the receding angle of drop 1+2+3 (θ_{r2}) is larger than the increase of the advancing angle of drop 1+2+3 (θ_{a2}). Before impact, the coalesced drop shows near-symmetrical shape (Figure 2c, 0.004 s), so $\theta_{a2} < \theta_{r2}$ in the dewetting process and the unbalanced surface tension force F_{d2} points in the RO direction.[23] F_{d2} makes the coalescent drop move along the RO direction, and at this stage, the ratchet angles ($\omega_1 < \omega_2$, $\omega_3 < \omega_4$) in these two opposite directions are determining factors for the introduction of F_{d2}.

After coalescence, the released surface energy in coalescence reaches a maximum, and it converts to the kinetic energy of the coalescent drop 1+2+3.[26−28] The kinetic energy (E_K) that drop 1+2+3 obtains is defined as

$$E_K = E_{S1} + E_{S2} - E_{S(1+2)} - E_V \quad (2)$$

where E_{S1} and E_{S2} are the surface energy of mother drops 1 and 2, $E_{S(1+2)}$ is the surface energy of coalescent drop 1+2, and E_V is the viscous dissipation due to coalescence (the diameter of the fog drops is smaller than 2.7 mm, so the gravity energy can be ignored). Given the same radius r of two drops, E_K is described as follows:[26]

$$E_K = \gamma\pi r^2\{(2 - 2^{2/3})(2 - 2\cos\theta) + [2^{2/3}\Psi_b(\Phi) - 2\Psi_a(\Phi)]\sin^2\theta\} - 64\pi\mu\sqrt{\frac{\gamma r^3}{\rho}} \quad (3)$$

where $\Psi(\Phi) = r_f\Phi\cos\theta_Y + \Phi - 1$ (r_f is the roughness ratio of wet surface area, Φ is the fraction of the solid area wetted by liquid, and θ_Y is Young's contact angle defined for smooth surface), $\Psi_a(\Phi)$ and $\Psi_b(\Phi)$ represent the $\Psi(\Phi)$ after and before coalescence, respectively, γ is the surface tension of water, ρ is the density of water, θ is the contact angle of the fog drop, and μ is the viscosity coefficient of water. On the basis of eq 3, in the ranges we have discussed ($1 < r_f \leq 3$, $100° < \theta_Y < 120°$), the coalesced drop on the surface with larger r_f and θ_Y will obtain more kinetic energy; thus it could move with high speed (supplementary discussions in the Supporting Information). In our case, the micro/nanostructure endows the butterfly wing with a large r_f, which is beneficial for the transport of the coalesced drop with high speed. So in the third stage, the unbalanced surface tension force and the released surface energy cooperatively lead to the apparent transport of the coalescent drop.

Living butterflies vibrate their wings in rotation mode with frequencies less than 20 Hz and amplitudes that are not larger than several centimeters.[11,12,29] When the amplitude is small, the motion of the wings can be regarded as vertical vibration. When the amplitude is large, the wings will tilt up and down with the insect body as the axis. Drops tend to move when the wings tilt down but tend to be pinned when the wings tilt up.[14] Therefore, even on the tilting wings, drops are more likely to move along the RO direction. On the basis of this phenomenon, if drops on vertical vibrating wings exhibit directional motion, drops on rotating wings can also move directionally regardless of the amplitude. So we applied vertical vibration on butterfly wings to imitate the vibration of living butterfly wings as far as possible. In our experiment, the vibration frequency ranged from 10 to 100 Hz and the amplitude ranged from 0.2 to 4 mm. The kinetic energy that the vibration machine produced is defined as $E_K \propto (1/2)\rho V(2\pi fA)^2$,[30,31] where ρ and V are the density and volume of the drop, respectively, f is the external forcing frequency, and A is half of the peak-to-peak amplitude of the vibration. According to this definition, the kinetic energy applied to the fog drops by our instrument is comparable to the living butterfly wings.

Interestingly, fog drops were propelled along the RO direction by the vibrating wings (Figure 4a). On the basis of the side view images (Figure 4b), we give an explanation for this directional transport. On vertical vibrating wings, influenced by the inertial force, the fog drop will spread (0.026 s) and recoil (0.030 s) cycle by cycle. Drops dewet easily along the RO direction while with difficulty against the RO direction because of the relative continuous three-phase contact line against the RO direction. Therefore, asymmetric contraction of fog drops happens and an unbalanced surface tension force pointing in the RO direction is introduced (0.030 s).[32] When the unbalanced surface tension force is large enough to overcome the retention force the entire drop encounters in the RO direction, the fog drop could move directionally in the horizontal direction (from 0.030 to 0.174 s).[33]

Figure 4c shows the relationship between the fog drop transport efficiency and vibration modes. Transport efficiency was estimated as the ratio of drop coverage on the butterfly wings after vibration to that before vibration. The vibration was continued for 1.37 s until all the moving drops had departed from the surface. This demonstrates that butterfly wings vibrating at 35 Hz, 4 mm, could efficiently drive fog drops along the RO direction.

In order to find the reason for the existence of this optimal vibration mode, we investigated the behaviors of single drops deposited on vibrating butterfly wings because deposited drops show similar movement activities to fog drops (Figure S5). The relationship between the vibration mode of butterfly wings and the velocity of deposited drops is shown in Figure S6. On butterfly wings vibrating at a frequency of 35 Hz, when the amplitudes were set at 2, 3, and 4 mm, the diameter range of the moving drops were 1.4−2.0, 1.2−2.2, and 0.9−2.4 mm, respectively. What's more,

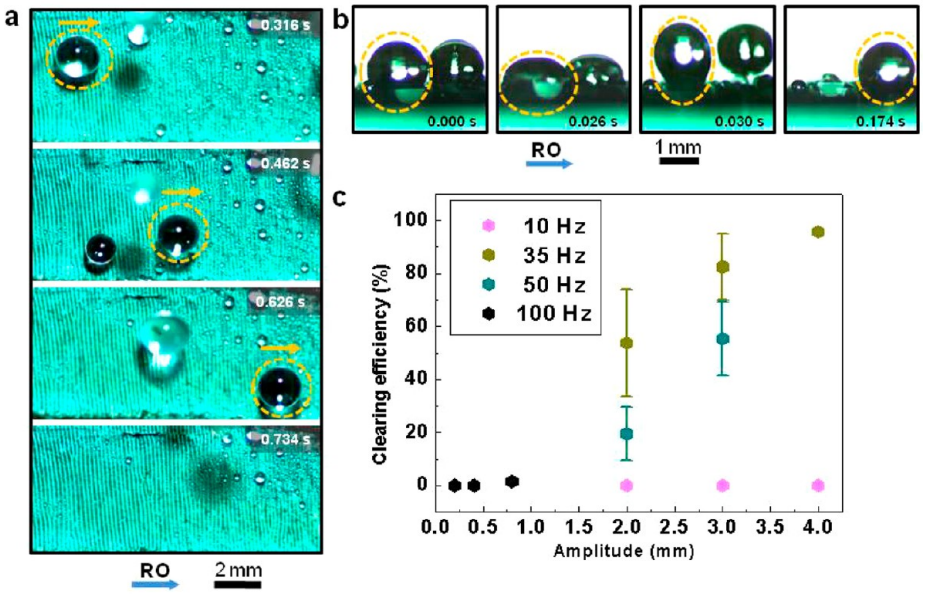

Figure 4. (a) Sequential images of top views showing the directional transport of fog drops on vibrating butterfly wings (video rate was 500 f/s; vibration mode was 35 Hz, 3 mm). Yellow arrows indicate the transport direction of the fog drops. (b) Sequential images of side views showing the directional transport of a fog drop (as shown in the yellow dotted circle) on vibrating butterfly wings (video rate was 500 f/s, vibration mode was 35 Hz, 3 mm). (c) Dot chart showing the fog drop transport efficiency of a vibrating butterfly wing.

the horizontal moving velocity of the drops with the same diameter almost increased with an increase of the amplitude. When the wings vibrated at other frequencies, the deposited drops showed no obvious motion.

Sessile drops will obtain more energy from a support plate that vibrates at a frequency approaching the natural harmonics of drop oscillation.[34] In our observation, when the butterfly wing was vibrated at 35 Hz, the mass center of the drop moved vertically to the support plate (Figure 4b, from 0.000 to 0.030 s). Hence this frequency is concluded as mostly approaching the rocking resonant mode of drops in our experiment,[34,35] and fog drops will obtain the maximum energy from the wings vibrating at 35 Hz. On a vertical vibrating surface, increasing the energy leads to the amplification of the contracting and impacting velocity of the drop and the difference between the receding and advancing contact angles is enlarged.[32] Hence fog drops will experience an amplified horizontal driving force, and the range of moving drop diameter is correspondingly enlarged. As for surface vibration at other frequencies, the horizontal force is not large enough to drive the drop and the reduction of drop coverage mainly results from drop coalescence triggered by vibration. Because the coalescence phenomenon occurred only among the fog drops with close neighbors, the drop transport efficiency of butterfly wings vibrating at other frequencies is small. At a constant frequency of 35 Hz, drops will get more energy as the amplitude increases.[30,31] Hence 35 Hz, 4 mm could propel drops in the large-diameter range, and wings vibrating at (or near) this vibration mode are able to transport fog drops efficiently.

As for living butterflies, keeping the wings light-loaded in fog is important for their flying flexibility. In order to find whether the directional fog drop transport ability contributes to the fog repellency of butterfly wings, we compare the moving behaviors of fog drops on butterfly wings with those on a silicon surface covered with vertical nanowires. The hydrophobicity of the silicon surface we fabricated was similar to that of a butterfly wing (Figure S7, the contact angle (CA) of the silicon surface was 150.7° ± 0.5° and the RA was 5.3° ± 0.8°), but fog drops on this isotropic surface moved randomly.[27] Considering the initial fog drops are smaller than the capillary scale (2.7 mm) and the influence of gravity can be neglected,[28,36] the transport of fog drops without the assistance of gravity is of significance in practical use. Therefore both of these surfaces were investigated horizontally. On butterfly wings, drops coalesced and moved off of the surface directionally (Figure 5a, from 240 to 360 s, drop 1+2, from 480 to 600 s, drop 3+4), while on the isotropic silicon surface, because the fog drops did not exhibit a uniform moving direction, the drop displacement was relative small and only a small portion of the fog drops moved off of the surface (*e.g.*, drops 2, 3, and 8 in Figure 5b). As condensation continued, the butterfly wings propelled more fog drops off (Figure 5c) and kept fewer drops on the surface (Figure 5d) compared with the silicon surface. In vibrating states, the butterfly wings propelled fog drops directionally away from the surface (Figure 4a), while the silicon surface just drove

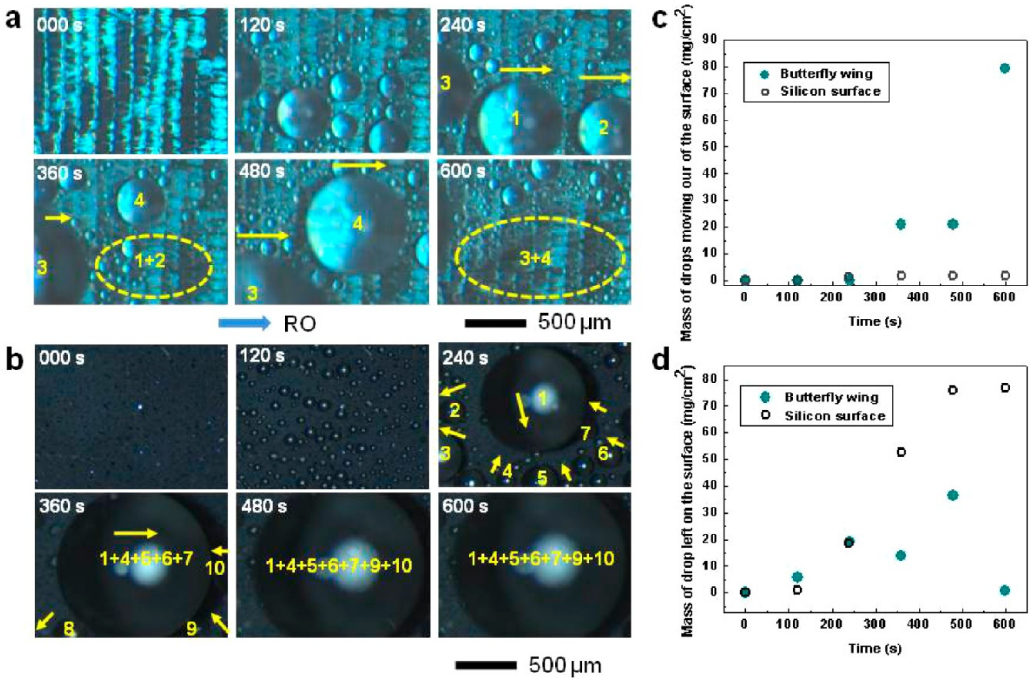

Figure 5. Sequential images showing the motions of fog drops on (a) anisotropic butterfly wings and (b) an isotropic silicon surface. The yellow arrows indicate the moving direction of fog drops. The yellow circles indicate the new clean places. Dot charts show the mass of fog drops moving off of (c) and left on (d) the butterfly wings and silicon surface per unit surface area.

the fog drops randomly and the horizontal displacement of the fog drops was small (Figure S8). So the butterfly wing exhibits excellent fog drop repellent property in both static and vibrating states. Additionally, armed with the directional fog drop transport ability, materials like butterfly wings may be able to drive fog drops to get together at a designed place away from the surface; thus the use of such kinds of materials might also be extended to water collection.

CONCLUSION

In summary, *M. deidamia* butterfly wings exhibit static and dynamic directional fog drop transport abilities. In static conditions, a superhydrophobic surface is essential for fog drops to have low retention force, which makes drop propulsion easy. Drop growth and coalescence on the asymmetric ratchet-like structure introduce an unbalanced surface tension force, which propels the fog drops directionally. In dynamic conditions, with the help of external energy, fog drops contract asymmetrically from the surface. An unbalanced surface tension force is introduced in this process, which endows the drop motion with directionality. Therefore, the asymmetric micro/nanostructures are indispensable in design materials used for directional fog drop transport in integrating static and dynamic modes.

EXPERIMENTAL SECTION

Sample Preparation of Butterfly Wings. Specimens of *Morpho deidamia* butterflies were purchased from Shanghai Dieyu Butterfly Office, China. The regions of butterfly wings without veins were prepared as the experimental samples. Samples of butterfly wings were cleaned with deionized water and then dried in the ambient environment before experiments.

Fabrication of Superhydrophobic and Isotropic Silicon Surface. The silicon wafers were cleaned by piranha solution (H_2SO_4 (97%)/H_2O_2 (30%) = 3:1) at 280 °C for 1 h. After that the wafers were cleaned by deionized water and blown dry by N_2. The Si substrates were etched in an etchant solution (HF = 4.6 mol/L and $AgNO_3$ = 0.02 mol/L) contained in a polytetrafluoroethene (PTFE) container for 2.5 min. After etching, the samples were put into 40% HNO_3 for 2 min to remove the deposited Ag dendrites. Then the samples were cleaned by deionized water and blown dry by N_2 again. After that the samples were put into a sealed container together with a piece of glass coated with 0.5 mL of fluoroalkylsilane. The container was then evacuated with a vacuum pump. After that the vacuum in the container was maintained for 12 h at 80 °C. Finally the superhydrophobic and isotropic silicon nanowire surfaces were obtained.

Observation of Directional Transport of Fog Drops on Static and Vibrating Butterfly Wings. A sample of butterfly wing (2 cm × 3 cm) pasted on a glass substrate was exposed to fog flow composed of microscale water beads generated by an ultrasonic humidifier (SC-4317, Beijing Yadu Science and Technology Co., China). The fog flow was generated at a rate of 30 cm/s, and the experiment temperature was 20 °C. The outlet of the fog flow was put diagonally above the sample (the angle between the surface and sample was about 53°) and vertically to the RO direction of butterfly wings with a vertical distance about 2 cm (as shown in Figure S9). An optical contact angle meter system with a CCD camera connected to desktop computer was used to record the behaviors of fog drops on a single scale. High-speed video (Phantom V9.1, Vision Research, USA) was used to observe the behaviors of drops that were larger than the size of a single scale. In the observation of fog drops on vibrating surfaces, the sample was pasted on the vertical vibration plate (GD-TP, Gaobang Experiment Equipment Co., China). When the vibration was applied, the fog flow was stopped to exclude the static drop

transport mechanism. The experiment with the same vibration mode was repeated three times. The average transport efficiency values were used as the final data. The average velocity of deposited drops that moved on butterfly wings for 1 cm was measured by software.

Observation of Behaviors of Fog Drops on Butterfly Wings and Silicon Surface. The butterfly wing and the silicon surface were put in the fog flow. The fog behaviors on these two surfaces were recorded by a Zeiss microscope (AxioCam Mrc 5, Carl Zeiss AG, Germany) with a CCD camera connected to a desktop computer. Then the mass of the fog drops removed from and left on the surfaces per unit surface area was calculated based on the radius of the drops.

Observation of Air Pockets Trapped between Fog Drops and Static Butterfly Wings. After exposure to the fog atmosphere for a certain time, the sample of butterfly wing (1 cm $\times$ 1 cm) retaining fog drops was put under the lens of a fluorescence microscope (CT-YGFM-30, Chengtong Precision Instrument Company of Shanghai, China). The light source was fluorescence light. We tuned the focus height to see the borderline of the fog drop clearly. Then we changed the focus height until the light area appeared between the fog drop and the butterfly wing.

Measurement of Contact Angles. Water contact angle and drop rolling-off angle were measured by an optical contact angle meter system (OCAMicro40, Dataphysics, Germany) at ambient temperature. Drops of 6.0 μL volume were deposited on the samples, and average CA and RA values at five different positions were taken as the final data.

Observation of the Butterfly Wings and Silicon Surface. The structures of the samples were obtained by an environmental scanning electron microscope (Quanta FEG 250, FEI, America) with a low-vacuum mode and an accelerating voltage of 10 kV.

Conflict of Interest: The authors declare no competing financial interest.

Acknowledgment. This work is supported by National Research Fund for Fundamental Key Project (2013CB933000, 2010CB934700), National Natural Science Foundation of China (21234001, 20973018), and Doctoral Fund of Ministry of Education of China (20101102110035, 20121102110035).

Supporting Information Available: This file contains Figures S1–S9, their captions, and supplementary discussions. This material is available free of charge *via* the Internet at http://pubs.acs.org.

REFERENCES AND NOTES

1. Ju, J.; Bai, H.; Zheng, Y.; Zhao, T.; Fang, R.; Jiang, L. A Multi-Structural and Multi-Functional Integrated Fog Collection System in Cactus. *Nat. Commun.* **2012**, *3*, 1247.
2. Zheng, Y. M.; Bai, H.; Huang, Z. B.; Tian, X. L.; Nie, F. Q.; Zhao, Y.; Zhai, J.; Jiang, L. Directional Water Collection on Wetted Spider Silk. *Nature* **2010**, *463*, 640–643.
3. Parker, A. R.; Lawrence, C. R. Water Capture by a Desert Beetle. *Nature* **2001**, *414*, 33–34.
4. Roth-Nebelsick, A.; Ebner, M.; Miranda, T.; Gottschalk, V.; Voigt, D.; Gorb, S.; Stegmaier, T.; Sarsour, J.; Linke, M.; Konrad, W. Leaf Surface Structures Enable the Endemic Namib Desert Grass *Stipagrostis sabulicola* to Irrigate Itself with Fog Water. *J. R. Soc. Interface* **2012**, *9*, 1965–1974.
5. Sun, T. L.; Feng, L.; Gao, X. F.; Jiang, L. Bioinspired Surfaces with Special Wettability. *Acc. Chem. Res.* **2005**, *38*, 644–652.
6. Bai, H.; Tian, X. L.; Zheng, Y. M.; Ju, J.; Zhao, Y.; Jiang, L. Direction Controlled Driving of Tiny Water Drops on Bioinspired Artificial Spider Silks. *Adv. Mater.* **2010**, *22*, 5521–5525.
7. Chen, X.; Wu, J.; Ma, R.; Hua, M.; Koratkar, N.; Yao, S.; Wang, Z. Nanograssed Micropyramidal Architectures for Continuous Dropwise Condensation. *Adv. Funct. Mater.* **2011**, *21*, 4617–4623.
8. Bai, H.; Ju, J.; Zheng, Y. M.; Jiang, L. Functional Fibers with Unique Wettability Inspired by Spider Silks. *Adv. Mater.* **2012**, *24*, 2786–2791.
9. Tian, X.; Chen, Y.; Zheng, Y.; Bai, H.; Jiang, L. Controlling Water Capture of Bioinspired Fibers with Hump Structures. *Adv. Mater.* **2011**, *23*, 5486–5491.
10. Daniel, S.; Chaudhury, M. K.; Chen, J. C. Fast Drop Movements Resulting from the Phase Change on a Gradient Surface. *Science* **2001**, *291*, 633–636.
11. Tanaka, M.; Matsumoto, K.; Shimoyama, I. Design and Performance of Micromolded Plastic Butterfly Wings on Butterfly Ornithopter. *IEEE/RSJ International Conference on Intelligent Robots and Systems*; Nice, France, 2008; IEEE: Piscataway, NJ, **2008**; pp 3095–3100.
12. Tanaka, H.; Hoshino, K.; Matsumoto, K.; Shimoyama, I. Flight Dynamics of a Butterfly-Type Ornithopter. *IEEE/RSJ International Conference on Intelligent Robots and Systems*; Edmonton, Alberta, Canada, 2005; IEEE: Piscataway, NJ, **2005**; pp 2706–2711.
13. Srygley, R. B.; Thomas, A. L. R. Unconventional Lift-Generating Mechanisms in Free-Flying Butterflies. *Nature* **2002**, *420*, 660–664.
14. Zheng, Y. M.; Gao, X. F.; Jiang, L. Directional Adhesion of Superhydrophobic Butterfly Wings. *Soft Matter* **2007**, *3*, 178–182.
15. Mei, H.; Luo, D.; Guo, P.; Song, C.; Liu, C. C.; Zheng, Y. M.; Jiang, L. Multi-Level Micro-/Nanostructures of Butterfly Wings Adapt at Low Temperature to Water Repellency. *Soft Matter* **2011**, *7*, 10569–10573.
16. Wanasekara, N. D.; Chalivendra, V. B. Role of Surface Roughness on Wettability and Coefficient of Restitution in Butterfly Wings. *Soft Matter* **2011**, *7*, 373–379.
17. Wagner, T.; Neinhuis, C.; Barthlott, W. Wettability and Contaminability of Insect Wings as a Function of Their Surface Sculptures. *Acta Zool.* **1996**, *77*, 213–225.
18. Gao, X. F.; Jiang, L. Water-Repellent Legs of Water Striders. *Nature* **2004**, *432*, 36.
19. Lafuma, A.; Quéré, D. Superhydrophobic States. *Nat. Mater.* **2003**, *2*, 457–460.
20. Verho, T.; Korhonen, J. T.; Sainiemi, L.; Jokinen, V.; Bower, C.; Franze, K.; Franssila, S.; Andrew, P.; Ikkala, O.; Ras, R. H. A. Reversible Switching between Superhydrophobic States on a Hierarchically Structured Surface. *Proc. Natl. Acad. Sci. U.S.A.* **2012**, *109*, 10210–10213.
21. Callies, M.; Quéré, D. On Water Repellency. *Soft Matter* **2005**, *1*, 55–61.
22. Extrand, C. W. Retention Forces of a Liquid Slug in a Rough Capillary Tube with Symmetric or Asymmetric Features. *Langmuir* **2007**, *23*, 1867–1871.
23. Chaudhury, M. K.; Whitesides, G. M. How to Make Water Run Uphill. *Science* **1992**, *256*, 1539–1541.
24. Yadav, P. S.; Bahadur, P.; Tadmor, R.; Chaurasia, K.; Leh, A. Drop Retention Force as a Function of Drop Size. *Langmuir* **2008**, *24*, 3181–3184.
25. Thoroddsen, S. T.; Takehara, K. The Coalescence Cascade of a Drop. *Phys. Fluids* **2000**, *12*, 1265–1267.
26. Wang, F. C.; Yang, F. Q.; Zhao, Y. P. Size Effect on the Coalescence-Induced Self-Propelled Droplet. *Appl. Phys. Lett.* **2011**, *98*, 053112.
27. Dorrer, C.; Rühe, J. Wetting of Silicon Nanograss: From Superhydrophilic to Superhydrophobic Surfaces. *Adv. Mater.* **2008**, *20*, 159–163.
28. Boreyko, J. B.; Chen, C. H. Self-Propelled Dropwise Condensate on Superhydrophobic Surfaces. *Phys. Rev. Lett.* **2009**, *103*, 184501.
29. Brodsky, A. K. Vortex Formation in the Tethered Flight of the Peacock Butterfly *Inachis io* L. (Lepidoptera, Nymphalidae) and Some Aspects of Insect Flight Evolution. *J. Exp. Biol.* **1991**, *161*, 77–95.
30. Boreyko, J. B.; Chen, C. H. Restoring Superhydrophobicity of Lotus Leaves with Vibration-Induced Dewetting. *Phys. Rev. Lett.* **2009**, *103*, 174502.
31. Boreyko, J. B.; Baker, C. H.; Poley, C. R.; Chen, C. H. Wetting and Dewetting Transitions on Hierarchical Superhydrophobic Surfaces. *Langmuir* **2011**, *27*, 7502–7509.
32. Reyssat, M.; Pardo, F.; Quéré, D. Drops onto Gradients of Texture. *Europhys. Lett.* **2009**, *87*, 36003.

33. Daniel, S.; Chaudhury, M. K. Rectified Motion of Liquid Drops on Gradient Surfaces Induced by Vibration. *Langmuir* **2002**, *18*, 3404–3407.
34. Daniel, S.; Sircar, S.; Gliem, J.; Chaudhury, M. K. Ratcheting Motion of Liquid Drops on Gradient Surfaces. *Langmuir* **2004**, *20*, 4085–4092.
35. Daniel, S.; Chaudhury, M. K.; de Gennes, P. G. Vibration-Actuated Drop Motion on Surfaces for Batch Microfluidic Processes. *Langmuir* **2005**, *21*, 4240–4248.
36. Rose, J. W.; Glicksma, L. R. Dropwise Condensation—The Distribution of Drop Sizes. *Int. J. Heat Mass Transfer* **1973**, *16*, 411–425.